Optik - International Journal for Light and Electron Optics 202 (2020) 163623

Contents lists available at ScienceDirect

Optik

journal homepage: www.elsevier.com/locate/ijleo

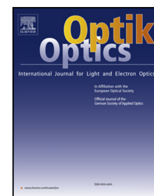

Original research article

Characteristic of fixed abrasive polishing for fused silica in anhydrous environment

Huiyang Tang, Wei Yang*, Wenjun Liu, Jinlei Ma, Xinyu Luo

School of Aerospace Engineering, Xiamen University, Xiamen 361005, China

ARTICLE INFO

Keywords:
Fixed-abrasive polishing
Fused silica
Roughness
Removal rate
Material removal mechanism

ABSTRACT

In order to overcome the randomness of free abrasive polishing (CMP), abrasive waste and the resulting hydration layer, this paper presents a fixed abrasive polishing technique in the anhydrous environment. We have achieved a stable polishing wheel sintering process. The pellet we made have applied to fused silica polishing.

It is found that the surface profile accuracy and roughness convergence speed are significantly improved comparing with the free abrasive polishing, and the pellet did not break and wears evenly. The influences of changing parameters including pressure, rotation speed on the material removal rate and surface roughness is examined. Removal rate does not increase with applied pressure and rotation speed, which is inconsistent with Preston's formula. The heat generated in machine process is paramount parameters determining removal efficiency. In order to get the most suitable processing temperature, We employed in-situ infrared camera and finite element analysis to test the temperature, which clarify the material removal does not increase with applied pressure and rotation speed in dry fixed abrasive polishing. Further, for testing the properties and stability of the pellet, the chips and polishing wheel were chemical analyzed using EDS and XRD, the results show a probable mechanism.

1. Introduction

The demand for high-precision optical components is increasing in the scientific and industrial fields such as civil optics, semiconductors, optical communications, large-scale laser nuclear fusion devices, and astronomical telescopes. Fused silica is widely used in manufacturing windows and shielding sheets due to its low coefficient of thermal expansion and large thermal inertial properties. The conventional machining is mainly “Precision / Ultra Precision Grinding + Deterministic CNC Polishing”, Free abrasive polishing technology currently used in the deterministic CNC polishing stage. It is mainly composed of three parts: polishing liquid, polishing pad and workpiece. Polishing liquid mainly use oxide compounds (usually rare earth & metal compounds include ceria, SnO2, TiO2, etc.) with lower hardness than glass as abrasives mixed with deionized water and chemical additives. The commonly used appropriate polishing pad encompass pitch, polyurethane, non-woven, Teflon, and so forth. The basic mechanism of material removal is to form an etched film on the surface of the workpiece under the action of the polishing solution, which reduces the surface hardness of the workpiece. The softer abrasive removes the film under the action of the mechanical action, and the exposed new surface is reformed and then removed. The material is eventually chemically-mechanically removed from Nowadays, the free abrasive polishing technology is maturely applied in the semiconductor industry, glass surface by repeating this process [1].

which widely used in the production and processing of mono-crystalline silicon and sapphire substrates for Planarization and

* Corresponding author.
E-mail address: yangwei@xmu.edu.cn (W. Yang).

https://doi.org/10.1016/j.ijleo.2019.163623
Received 28 July 2019; Accepted 13 October 2019
0030-4026/ © 2019 Elsevier GmbH. All rights reserved.

polishing. Notwithstanding the widespread use, there are still many shortcomings in polishing process [2]. 1. Free abrasive polishing will produce a hydrated layer of a few nm to several hundred nm on the surface of the glass, the optical properties of glass are reduced due to the essential differences between the mechano-chemical properties of the hydrated layer and the glass bulk material; 2. It is hard to precisely predict the removal of material that is subject to motion of abrasives, because the movement of abrasives is stochastic in loose abrasive polishing; 3. Polishing pads and polishing materials degrade and wear during polishing, and need to be regularly trimmed at regular intervals, but trimming is a time-consuming task;4. It is reported that merely 0.5% of abrasives take part in material removal in loose abrasive, implying that most abrasives are actually unused and a huge portion of polishing material is wasted.

In order to overcome the shortcomings of the traditional free abrasive polishing method, hence some institutes and organizations have turned to fixed abrasive polishing. Professor Stephen D. Jacobs of the University of Rochester in the United States developed a cerium oxide fixed abrasive polishing technique, which could reduce the roughness rms of fused silica from 400 nm to 1.5 nm in 1 h [3]. Ukrainian Yuriy D. Filatov scholars used the cluster model to study the removal mechanism of optical materials on the fixed abrasive, and further explained the removal mechanism of the fixed abrasive polishing. Prof. L. Zhou from Ibaraki University in Japan has manufactured the prototype of a cerium oxide fixed-abrasive pellet that can be utilized to polish mono-crystalline silicon wafer without defect processing [4]. Based on this technology, Professor Yongbo Wu and Yaguo Li successfully introduced the assistance of two-dimensional ultrasonic to polish fused silica in anhydrous environment [5], Chenghu Zhou et al. [6] investigated the potential influence of various liquids and the different kinds of pellets on the polishing process as well as the wear of pellet in ultrasonic assisted and conventional processes. These studies have successfully transformed the traditional CMP 3-object system into a 2-object system. Nevertheless, these studies not only have complicated preparation processes for polishing wheels, but also use deionized water as a coolant during processing, which inevitably form a layer of sol-gel that is much softer than bulk glass.

Based on the previous research, this paper is devoted to the process of formulating a stable fixed abrasive polishing wheel. Then we applied the pellet to the machining of fused silica in a waterless environment to obtain a water-free, defect-free high-quality surface, which ultimately enables deterministic control of the bonded abrasive polishing technology. The main parameters involved in the material removal rate and surface roughness in the polishing process such as downward load and rotation speed will be investigated. Additionally, for testing the properties and stability of the pellet, the chips and polishing wheel were investigated by chemical analysis,

2. Experimental

2.1. Preparation of polishing wheel

The pellets were selected to use CeO2 with hardness equivalent to the fused silica as abrasive, which can reduce mechanical damage caused by abrasive polishing. The pellets are composed of 70% ceria (Average particle size 2.0 ~ 2.5um) and 15% binding material-phenolic resin (curing temperature is 150 °C); In addition, there are 15% hollow glass micro-spheres(with diameter of 10 ~ 250um) as additives [7]. The additives can be broken up during the process to accommodate polishing debris. The broken micro-spheres hardness is greater than that of the phenolic resin, causing the phenolic resin to be scraped off, which is advantageous for further exposure of the cerium oxide abrasive.

After uniformly mixing according to the above ratio, the powder is filled and pressed in a Ø13 mm cylindrical mold, then, it is sintered in the furnace with a certain temperature rise program as shown in Fig. 1(a). The formed pellet is shown in Fig. 1(b). In order to ensure uniform heating and heat dissipation inside the polishing wheel pellets, a stepwise lifting is adopted during the heating and cooling process.

2.2. Experimental procedure for polishing

In order to study dependencies of downward load and rotation speed on the removal rate and surface roughness, five different sets of parameters were tested in a circular fused silica sample with dimension of Φ50 mm × 10 mm and initial surface roughness of ~ 200 nm Ra as shown in Table 1. The experimental apparatus as schematically illustrated in Fig. 2.The apparatus incorporates of three parts: tool for bonding cerium pellet, four pieces of iron for fixing the work-piece bonded to the aluminum plate, CNC machine.

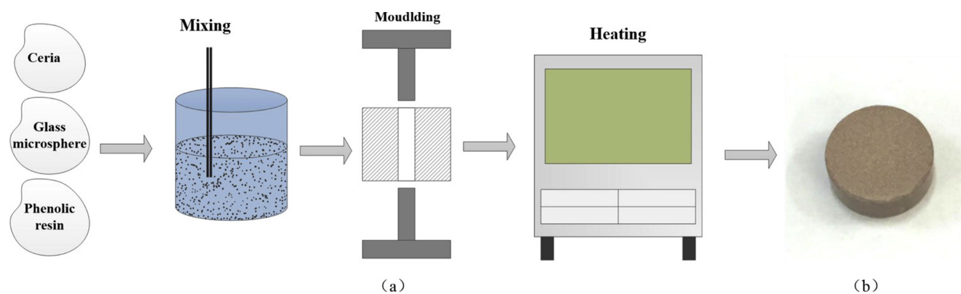

Fig. 1. Schematic of the pellet. (a) the pellet production process. (b) polishing pellet.

Table 1
The experimental parameters.

Pellets		Dimension Abrasive	Ø13 mm×5 mm CeO2
Stroke in X direction		L	3 mm
Eccentricity		e	32 mm
Velocity of oscillation		V_x	2 mm/s
Experimental NO.	Downward load	Rotating speed of Pellets	Rotating speed of sample
1	50 kPa	95 rpm	105 rpm
2	50 kPa	145 rpm	155 rpm
3	50 kPa	195 rpm	205 rpm
4	25 kPa	95 rpm	105 rpm
5	70kPa	95 rpm	105 rpm

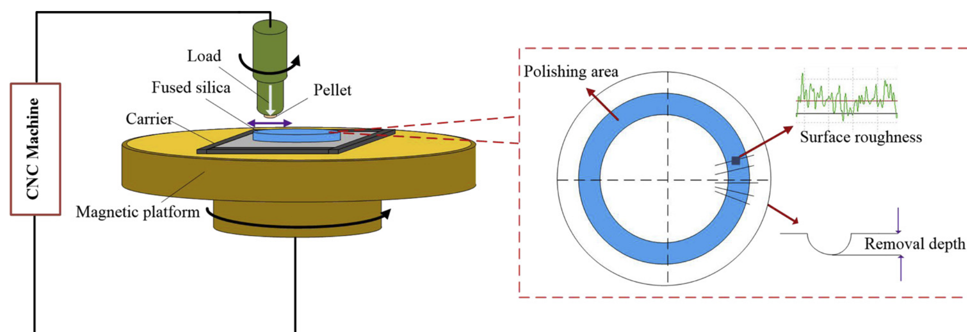

Fig. 2. The experimental apparatus and evaluation method for surface roughness and material removal.

The CNC machine consists of a magnetic platform for rotating, a unit for the right or left motion, a mechanism for the vertical feed motion. The downward pressure is controlled by relative displacement in Z-direction, which determined quantitatively with a dy-namo-meter. The machined region was an annul-us offset ~32 mm away from the center of the fused silica sample, the pellet rotates in the same direction and reciprocates in the X direction at a speed of 2 mm/s and a stroke of 6 mm. The speed of work-piece and the speed of pellet are different, which can prevent the surface of the work-piece from being pitted due to periodic motion [8]. The material removal was tested with a contact stylus pro-filer (Taylor Hobson Form PGI1240, UK). The surface roughness and material removal were checked every 10 min after cleaning the surface with ethanol. Each sample was polished for 7 times, i.e. 70 min in total. Before each experiment, pellet was trimmed by an alumina wheel with a median diameter of 9um to ensure that the abrasive particles were fully exposed. In order to ensure the removal depth and roughness measurement accuracy, the measurement area selects the area where the fused silica is first processed in the region with the lowest roughness after the first 10 min processing. All the experiments were conducted without adding any fluids during the polishing process unless otherwise specified. Five measurements of surface roughness were taken in the relatively scattered positions as shown in Fig. 2. The surface roughness is the average of the five measurements.

2.3. Chemical analysis

In order to test the properties and stability of the pellet during processing, polishing pellets and chips was made essential chemical analysis, EDS, and XRD included. The goal is to confirm the content of various major elements in the sample, the type of compound, and the chemical bonds contained.

3. Results and discussion

3.1. Material removal rate and surface roughness

Fig. 3(a),(c) shows the material removal rate and the sample roughness with different rotation speed. Fig. 3(b),(d) shows the material removal rate and the surface roughness with different downward load.

When the pressure is 50 kPa as shown in Fig. 3(a). MRR (150 rpm) > MRR(100 rpm) ≈ MRR(200 rpm).

When the pressure is 50 kPa as shown in Fig. 3(b), MRR_{50kPa} > MRR_{75kPa} > $MRR_{25kP.}$ It is noteworthy that increasing the rotation speed and applied pressure would not increase the material removal rate, which does not follow common creeds held by polishing community that material removal rate should ascend with the elevated pressure and speed [9]. The reason may be that greater

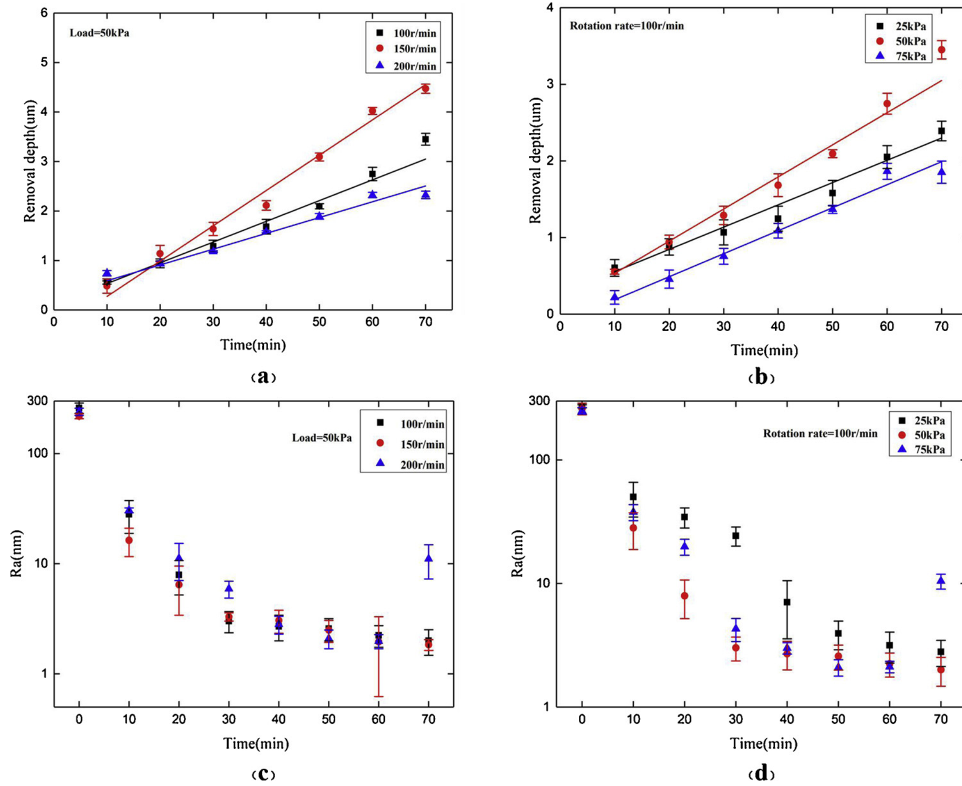

Fig. 3. Material removal rate versus polishing time under varied processing parameters. (a)The polishing process cannot progress under rotation rate = 200 r/min at 60 min.(b) The polishing process cannot progress under load = 75k at 60 min.(c)The pellet was burnt under rotation rate = 200 r/min at 60 min, which induce the deterioration in surface quality. (d)The pellet was burnt under load 75 kPa at 60 min, which induce the deterioration in surface quality.

pressure and speed cause the high temperature in the processing area. The attributes of pellet will modify under such high temperature, which results the decrease in material removal. Fig. 4 shows the pellet have been burnt under the load of 75kpa and the rotation speed of 200 rpm at 60 min. On this occasion, the polishing process cannot progress. If decreasing the load and rotation rate, it is found that the material can be removed without any abnormalities. Hence, it is reckoned that there exists a threshold for the applied load and speed.

Surface roughness increased after 60 min due to burns on the pellet surface under load of 75kpa and speed of 200 rpm as shown Fig. 4. The blackish substance of surface is an obstacle to polishing. In our experiments, the threshold of removal rate and the best surface roughness were under load 50 kPa, speed 150 rpm, the material removal rate reaches maximum value: about 4.2 um/h and the surface roughness Ra = 1.7 nm as shown Fig. 5(a). Fig. 5(b) shows surface morphology of fused silica after polished. (Keyence VHX-5000), which no cracks, scratches and pits are present in polished surface.

3.2. Chemical feature of polishing process

Fig. 6 shows the results of EDS,the main components borosilicate glass micro-spheres are Si and O. Ce and O elements are the main components of pellet powder. Table 2 shows the percentage of each element, the main elements of pellets powder and chips are

Fig. 4. The burnt surface of pellet.

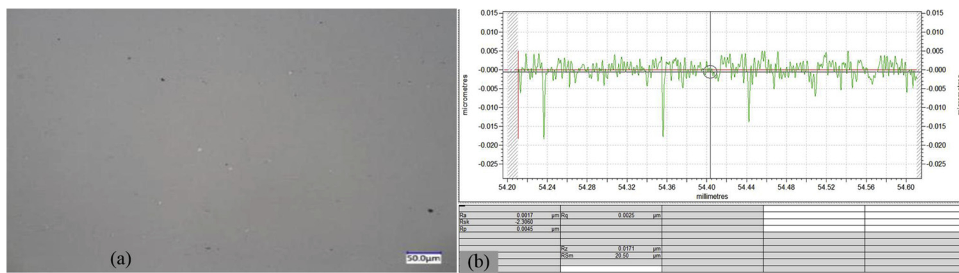

Fig. 5. Surface morphologies and the surface roughness.

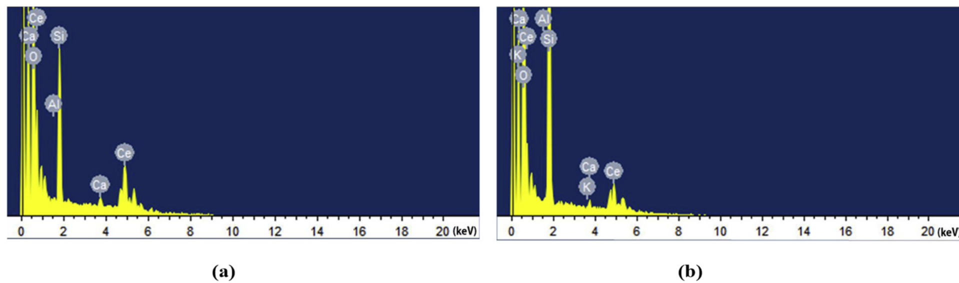

Fig. 6. EDS of pellet powder(a)and chips(b). Compared with the pellets, the proportion of silicon is increased, and the proportion of Ce is reduced in the chips.

Table 2
Contrast diagram of element weight percentage of pellet powder and grinding chips.

Element	Percentage of pellet powder	Percentage of chips
O	32.32	43.98(↑)
Al	0.06	0.04
Si	11.42	22.52(↑)
Ca	1.85	1.08
Ce	54.34	32.38

O, Al, Si, Ca and Ce. What we are most concerned about is the percentage change of Si and O, which is the main element of fused silica. Obviously, the proportion of Si and O element is increased, the proportion of Ce element is reduced in the chips. It can be recognized that Si element has been transferred to chips. Moreover, Fig. 7 shows significant diffraction peaks in the pellet powder and chips, which caused by crystal CeO2. Fig. 7 shows that amorphous materials are also present in the chips, which including glass micro-spheres and fused silica. the EDS and XED spectra evidence that material is removed in an anhydrous environment.

Fig. 8 shows the infrared spectrum analysis of fused silica, polishing wheel and debris. The Si-O bond of fused silica has a distinct absorption peak around 1109. The bond of the borosilicate glass micro-spheres of the pellet has a distinct absorption peak around1080. In the processed chips, the Si-O bond has a distinct absorption peak around 1078. It is demonstrated that the Si-O /cm1109 has shifted to 1078/cm, which results from the formation of Si-O-Ce bond [10].

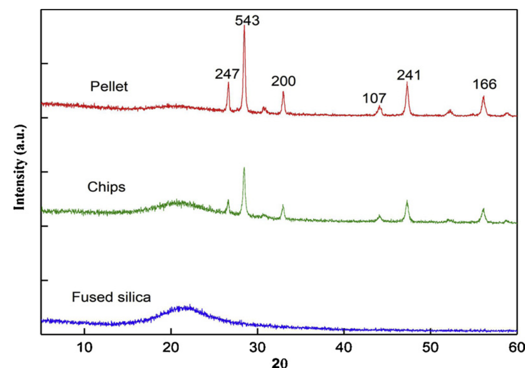

Fig. 7. XRD analysis of fused silica powder, pellet powder and chips.

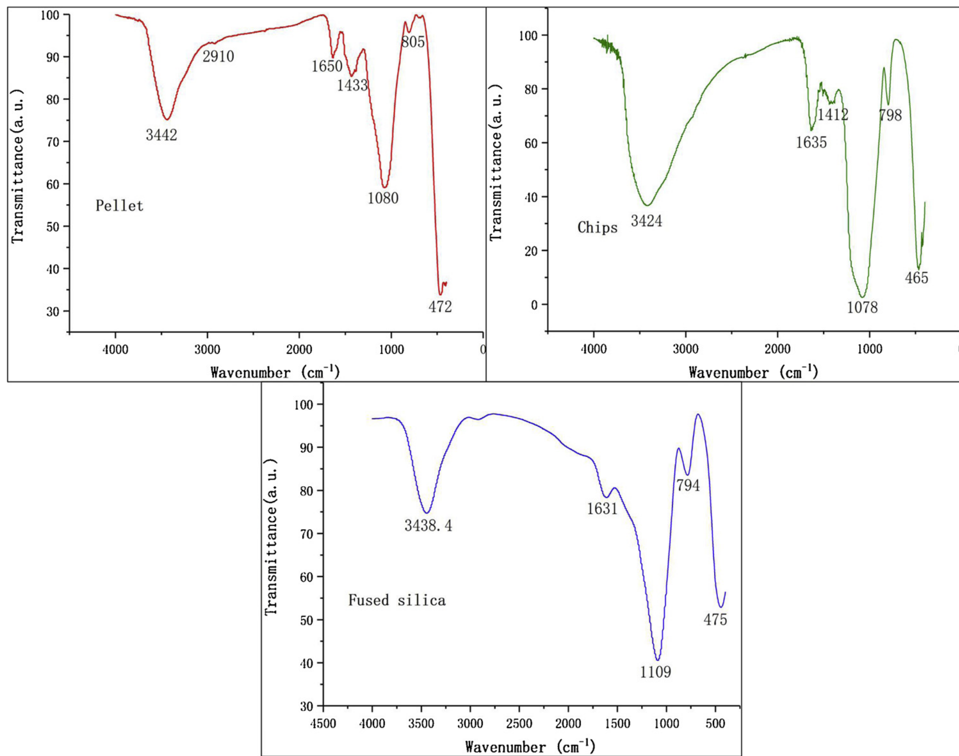

Fig. 8. Infrared spectra results of fused silica powder, pellets and chips. The shift of 1099/cm (Si–O) to 1085/cm indicates the potential formation of Si–O–Ce.

Cook [11] and K. Osseo-Asare [12] found that the processing of fused silica with a polishing solution containing CeO2 abrasive particles is an adsorptive material removal process. In the water processing environment, the Ce atom in CeO2 reacts with H2O to form a hydroxide of Ce as shown Eq. (1). Then the hydroxide of Ce reacts with silanol (a hydrate produced by the reaction of SiO2 with water) to form Ce-O-Si see Eq. (2). the Ce-O-Si bond energy is greater than the Si-O-Si bond energy. With the relative movement of CeO2, SiO2 is taken out from the fused silica to achieve material removal.

$$= Ce - O - Ce \equiv + H_2O \rightarrow \; = Ce - OH + HO - Ce = \tag{1}$$

$$= Ce - OH + \; HO - Si \equiv \; \rightarrow \; = Ce - O - Si \equiv + H_2O \tag{2}$$

On the results of the above chemical testing. the material removal process is reckoned. In the dry polishing environment, the Ce atom in CeO2 is relatively unstable. The center of the CeO2 abrasive is a tetravalent Ce atom and the surface is a trivalent Ce atom. The Ce atom bonds with Si-O bond in solid-state phase under the circumstances of high pressure to form Ce-O-Si bond as shown Eq. (3), whose strength is greater than the Si-O-Si bond, then the material is torn away from fused silica as a lump on account of strong shear force and this way the glass material is removed. The surface trivalent cerium oxide is oxidized to tetravalent CeO2 in an air-rich oxygen environment (Eq. (4)). Fig. 9 shows the mechanism in dry polishing of Fused silica with ceria. The main component in the final processed chips is a mixture of CeO2 and SiO2. The results of t chemical experiments are consistent with scholar [4], which confirms that the pellets we made can be applied to the processing of fused silica.

$$= Ce - O - Ce \equiv + = Si - O - Si \equiv \rightarrow 2 = Ce - O - Si \equiv \tag{3}$$

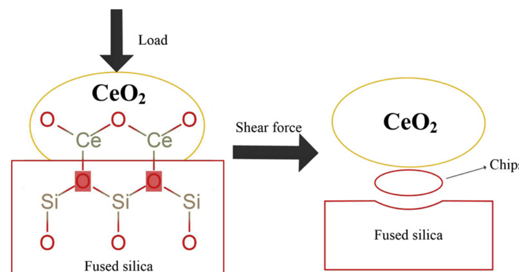

Fig. 9. The mechanism in dry polishing of fused silica with ceria.

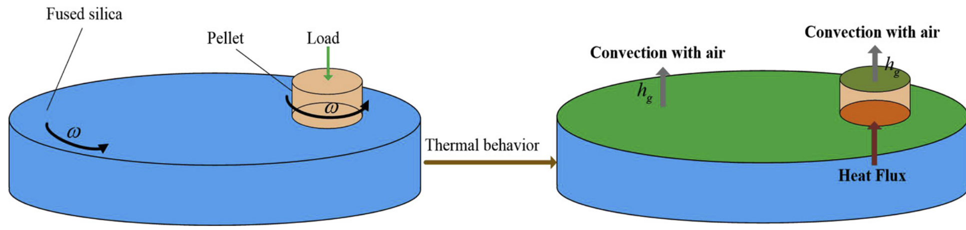

Fig. 10. Simplified scheme of simulation.

$$Ce_2O_3 + \frac{1}{2}O_2 \rightarrow 2CeO_2 \quad (4)$$

3.3. The temperature in machining Fused silica

3.3.1. Element analysis for temperature in process of polishing

In our experiment, increasing the downward load and rotation rate would not promote MRR(material removal rate). The reason may be that greater pressure and rotation rate will induce greater temperature rise. The attributes of pellet will modify under such high temperature, which results the decrease in material removal. It is necessary for us to tentatively evaluate temperature in fixed-abrasive polishing process. we analyzed the polishing temperature using ANSYS Workbench. The thermal behavior due to the motion of the machining process is converted into heat transfer [13] between the pellet and the work-piece and the convection between air and pellet, work-piece shown Fig. 10.

There is a stable heat flux (μpv) at the contact surface between the pellet and the work-piece, where μ is the coefficient of friction, p is the contact pressure (which may vary within the contact area), v is the sliding velocity. The maximum temperature of contact area was predicted by a finite element analysis A typical result is shown in Fig. 11. For the case of the pellet made from CeO2 with properties given in Table 3. It is assumed that a uniform heat flux $q = 1008W/m^2$ enters the pellet and work-piece, which corresponds to the process parameter rotation rate: 50 rpm, load:200k. The contact zone is assumed to be held at a constant room temperature of 21°C. It demonstrated that the maximum temperature in the contact zone is 95.942 °C, occurring at the center of the contact zone at the base of the pellet (Table 3).

In order to obtain the exact value of v, the motion process was analyzed shown in Fig. 12. Suppose that the pellet and the work-piece rotate at ω rate, $o_1o_2 = e$, e is annulus offset 32 mm away from the center of the sample. Suppose a point P of the pellet, whose initial position is on the o_1o_2 line. $O_2P = r_p$, $O_2X_2Y_2$ is a fixed coordinate system, $O_1X_1Y_1$ is the coordinate system fixed on the work-piece. After t time, the coordinates of point p in the coordinate system are:

$$x_2p = r_p\cos\omega t \quad (5)$$

$$y_2p = r_p\sin\omega t \quad (6)$$

$O_1X_1Y_1$ has been turned over ωt, which becomes $O_1X_1'Y_1'$ shown in Fig. 15b. The coordinates of P in the $O_1X_1'Y_1'$ are:

$$x_1'p = e\cos\omega t \quad (7)$$

$$y_1'p = e\sin\omega t \quad (8)$$

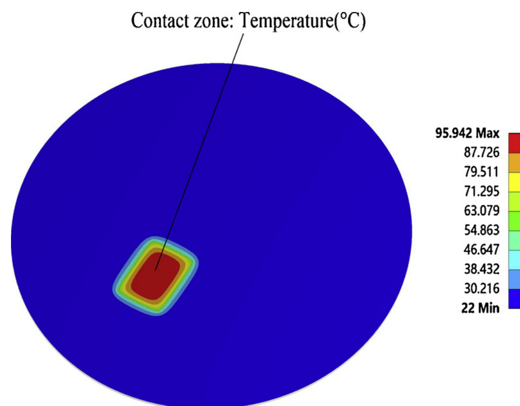

Fig. 11. Results of finite element analysis (using ANSYS Workbench) of contact zone between pellet mainly made from CeO2 and Fused silica. The initial temperature was held 21 °C. Convection coefficient with air h_g from the surface was $10W/m^2{\cdot}°C$. Maximum temperature is 95.942 °C at center of bottom surface of pellet.

Table 3
Material properties of Fused silica and CeO2 materials used in this study.

Material/property	Fused silica	CeO2
K Thermal conductivity (W/m· °C)	1.3	0.4
ρ Density(g/cm3)	2500	3980
C_p Specific heat(J/(kg·°C)	800	61.789

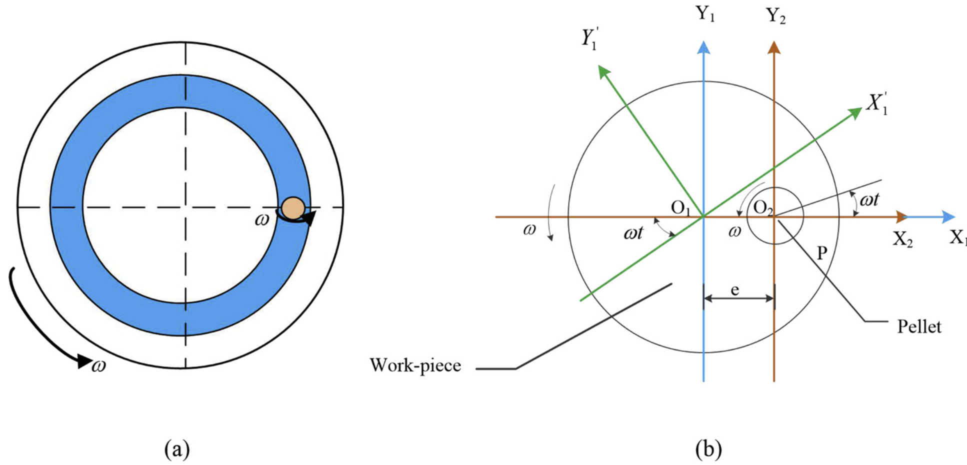

Fig. 12. Motion diagram of polishing process.

Then the speed of P on the pellet relative to the work-piece is:

$$v = \sqrt{\left(\frac{dx_1'p}{dt}\right)^2 + \left(\frac{dx_2'p}{dt}\right)^2} \tag{9}$$

Substituting (7) and (8) into (9):

$$v = \omega e \tag{10}$$

To solve the heat flux q, it is necessary to obtain the friction coefficient u. The value of the friction coefficient of pellet on work-piece is not constant during the polishing process, which is affected by the roughness of the contact surface [14], the load and the rotation rate [15]. Due to the difficulty of testing and the lack of sufficient experimental conditions, it was assumed a range between 0.01 and 0.05, a reasonable value for dry polishing of fused silica [16]. And it is difficult to test the thermal conductivity of pellet. it was assumed a range between 0.01 and 0.05. Resulting contact maximum temperatures of different processing parameters are shown in Fig. 13. It is apparent that elevating either rotation rate or downward force will increase the maximum temperature. Elevating rotation rate makes greater difference than downward force to temperature.

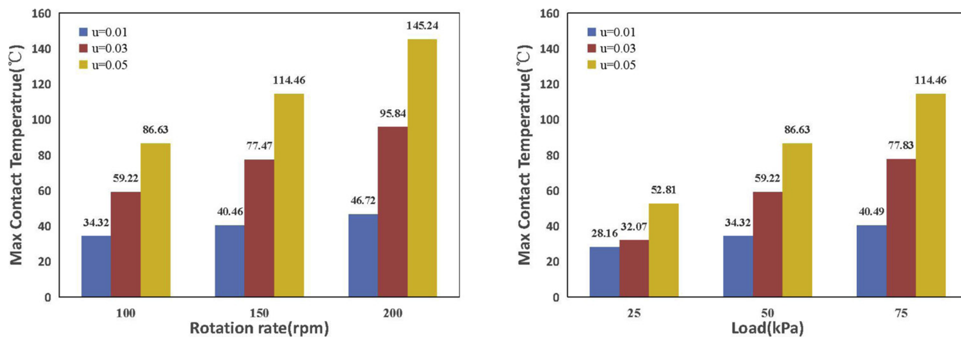

Fig. 13. Predicted maximum contact temperature of different friction coefficient (using ANSYS Workbench),which a heat flux is calculated by $q = \mu p v$, the figure on the left is the maximum temperature of different rotation rate at load of 50 kPa, the right is the maximum temperature of increasing load at rotation rate of 100 rpm.

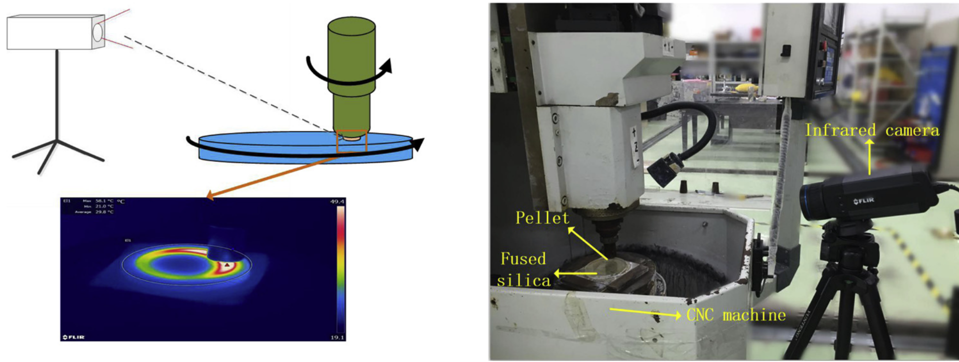

Fig. 14. Sketch of temperature measuring system.

3.3.2. Temperature measuring of polishing

In order to verify the simulation and obtain the temperature during processing, we employed in-situ infrared camera (A325sc, Fourier CO. LTD, America)to test the temperature (see Fig. 14).

It can be seen from Fig. 15 that the stage of t = 0 ~ 10 s is the unprocessed state, and the surface temperature of the work-piece is room temperature 21 °C, then the temperature increased fast in several seconds and final temperature reached a plateau in ~ 1 min when the heat generation and dissipation balanced. Increasing either rotation rate or downward force will increase the maximum temperature as shown Fig. 16. It is apparent that elevating rotation rate makes greater difference than downward force to temperature. The trends are similar with the simulation that increasing load and rotation rate will increase temperate shown in Fig. 17. The simulated temperature is higher than the experimented, which may be because the infrared camera cannot detect the temperature at the time of contact. It can be inferred that the pellets can only work normally below 80 °C.

It is worth mentioning that the temperature rise in the processing zone promotes the chemical reaction between cerium oxide and fused silica as the rotational speed increases from 100 rpm to 150 rpm. Therefore, the material removal rate is increased. However, when the rotation speed is increased from 150 rpm to 200 rpm, which will induce greater temperature rise. The pellet cannot stand such high temperature and chemical reactions cannot be carried out efficiently, which will induce pellet is burnt. Therefore, the removal efficiency is reduced. However, It can not achieve maximum removal when the pressure from 25 kPa to 75 kPa, which did not reach the optimum reaction temperature of pellet and fused silica. When the pressure = 75kpa, the grinding wheel was burned again. In Summary: the process parameters affect the temperature during processing, and the temperature affects the removal efficiency. At low temperature, it is difficult for ceria to chemically react with fused silica. At high temperature, the pellet cannot stand such high temperature and chemical reactions cannot be carried out efficiently. Hence, proper temperature during processing is important to improve removal efficiency, which promotes chemical reactions between pellet and fused silica. In our experiment, the proper temperature is around 58 °C, which Corresponds process parameter is load = 50 kPa, rotation rate = 150 rpm.

4. Conclusions

This paper presents fixed abrasive polishing technique in anhydrous environment, which could overcome the randomness of free abrasive polishing (CMP), abrasive waste and the resulting hydration layer. It was found that:

- It is determined that the preparation route of the polishing wheel is “weighing + stirring + cold pressing + thermosetting”, and

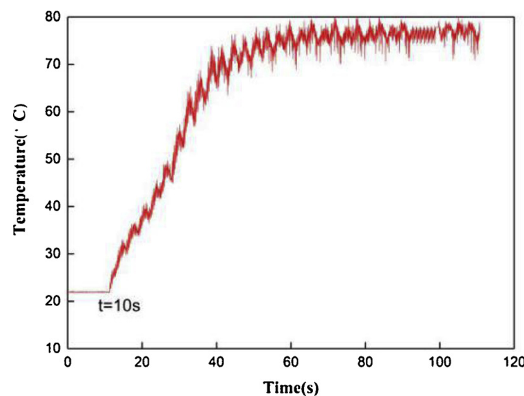

Fig. 15. Temperature rise for fused silica.

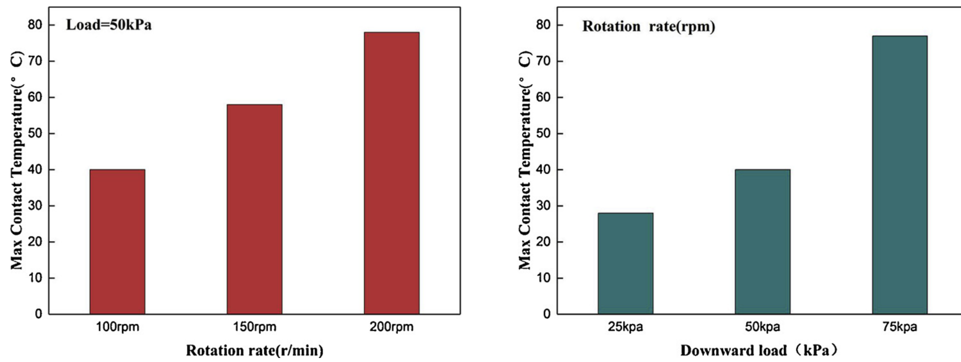

Fig. 16. The temperature of fused silica polishing versus and rotation rate downward force.

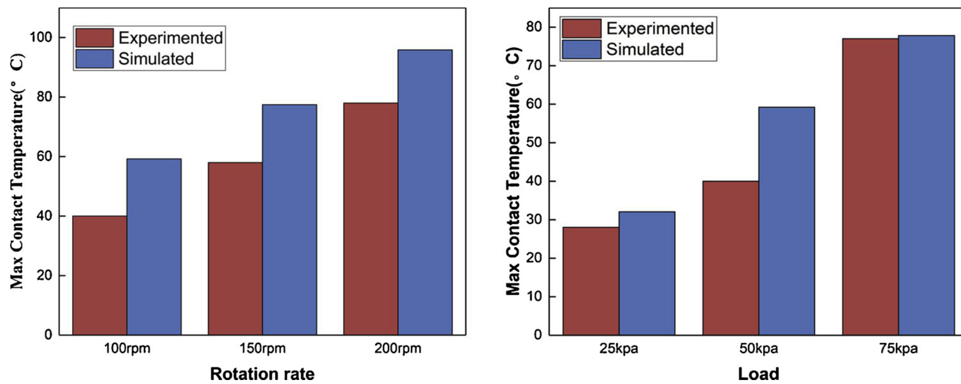

Fig. 17. The experimented and simulated temperature. (the left load = 50kpa,the right rotation = 100 rpm). The simulated temperature is little higher than the experimented.

the optimum composition ratio of the pellet is determined to be cerium oxide: phenolic resin: hollow glass microspheres = 7: 1.5: 1.5.

- The removal mechanism of the processing method is explored by the chemical analysis. The main components of the final processed product is the mixture $CeO2$ and $SiO2$, which confirms that the pellets we made can be applied to the processing of fused silica. The effects of pressure and rotation speed on removal efficiency and surface quality were clarified, the optimum processing parameters of this technology in the waterless environment is 50 kPa, 150 rpm, the surface roughness Ra was less than 2 nm, and the processing depth could be achieved. 4.2um/h, high quality surface with no water layer on the surface.
- The temperature was systematically inspected by IR pyrometer. The actual processing temperature is between 28 °C and 80°C, which explains the reason that the removal efficiency does not follow Preston's rule.

References

[1] F.B. Kaufman, Chemical-mechanical polishing for fabricating patterned W metal features as chip interconnects, J. Electrochem. Soc. 138 (11) (1991) 3460.
[2] J.Y. Choi, H.D. Jeong, A study on polishing of molds using hydrophilic fixed abrasive pad, Int. J. Mach. Tools Manuf. 44 (11) (2004) 1163–1169.
[3] B.E. Gillman, S.D. Jacobs, Bound-abrasive polishers for optical glass, Appl. Opt. 37 (16) (1998) 3498.
[4] L. Zhou, H. Eda, J. Shimizu, et al., Defect-free fabrication for single crystal silicon substrate by chemo-mechanical grinding, CIRP Ann. Manuf. Technol. 55 (1) (2006) 313–316.
[5] Y. Li, Y. Wu, L. Zhou, et al., Vibration-assisted dry polishing of fused silica using a fixed-abrasive polisher, Int. J. Mach. Tools Manuf. 77 (1) (2014) 93–102.
[6] C. Zhou, Q. Zhang, C. He, et al., Function of liquid and tool wear in ultrasonic bound-abrasive polishing of fused silica with different polishing tools, Opt. – Int. J. Light Electron. Opt. 125 (15) (2014) 4064–4068.
[7] L. Wenjun, Y. Wei, G. Yinbiao, Research on the characteristic of bounded abrasive polishing for fused silica glass in anhydrous environment, High Power Laser Part. Beams (2018).
[8] Y. Li, J. Hou, Q. Xu, et al., The characteristics of optics polished with a polyurethane pad, Opt. Express 16 (14) (2008) 10285–10293.
[9] F.W. Preston, The structure of abraded glass surfaces, Tans. Opt. Soc 23 (3) (1922) 141–164.
[10] Y. Li, Y. Wu, L. Zhou, et al., Chemo-mechanical manufacturing of fused silica by combining ultrasonic vibration with fixed-abrasive pellets, Int. J. Precis. Eng. Manuf. 13 (12) (2012) 2163–2172.
[11] L.M. Cook, Chemical processes in glass polishing, J. Non Cryst. Solids 120 (1) (1990) 152–171.
[12] K. Osseo-Asare, Surface chemical processes in chemical mechanical polishing relationship between silica material removal rate and the point of zero charge of the abrasive material, J. Electrochem. Soc. 149 (12) (2002) G651–G655.
[13] N. Laraqi, N. Alilat, J.M.G.D. Maria, et al., Temperature and division of heat in a pin-on-disc frictional device—exact analytical solution, Wear 266 (7) (2009) 765–770.
[14] A. Kumar, T. Staedler, X. Jiang, et al., Effect of normal load and roughness on the nanoscale friction coefficient in the elastic and plastic contact regime, Beilstein J. Nanotechnol. 4 (1) (2013) 66–71.
[15] Y.L. Sun, D.W. Zuo, Y.W. Zhu, et al., Effect of ice counterparts on the friction behavior of single crystal silicon wafer, Adv. Mat. Res. (2008) 167–172.
[16] A.L. Yurkov, V.N. Skvortsov, I.A. Buyanovsky, et al., Sliding friction of diamond on steel, s and without lubricants, J. Mater. Sci. Lett. 16 (16) (1997) 1370–1374.